Optical characterization of InN layers grown by high-pressure chemical vapor deposition

M. Alevli,[a] R. Atalay, G. Durkaya, A. Weesekara, A. G. U. Perera, and N. Dietz
Department of Physics and Astronomy, Georgia State University, Atlanta, Georgia 30303

R. Kirste and A. Hoffmann
Tecische Universität Berlin, Germany

(Received 9 November 2007; accepted 17 March 2008; published 1 July 2008)

The optical properties of InN layers grown by high-pressure chemical vapor deposition have been studied. Raman, infrared reflection, and transmission spectroscopy studies have been carried out to investigate the structural and optical properties of InN films grown on sapphire and GaN/sapphire templates. Results obtained from Raman and IR reflectance measurements are used to estimate the free carrier concentrations, which were found to be varying from mid 10^{18} to low 10^{20} cm^{-3}. The values for free carrier concentrations are compared to optical absorption edge estimates obtained from optical transmission spectra analysis. The analysis shows that optical absorption edge for InN shifts below 1.1 eV as the free carrier concentration decreases to low 10^{18} cm^{-3}. © *2008 American Vacuum Society.* [DOI: 10.1116/1.2908736]

I. INTRODUCTION

The controlled incorporation of individual constituents in III-nitride alloys $(Ga_{1-y-x}Al_yIn_x)N$ and formation of heterostructures of them is crucial for development and fabrication of multitandem solar cells, advanced high-speed optoelectronic structures, monolithic integrated spectral tunable light sources and high-efficient photovoltaic converters[1,2] operating in wide spectral range.[1,3] This material system is stable for applications under high radiation exposures and high temperature environments.

In conventional deposition techniques, the large thermal decomposition pressure of InN limits the growth temperatures at and below 600 °C, which is at least 200 °C lower compared to gallium-rich GaInN process conditions.[4] Therefore, the process window for InN needs to be enlarged or shifted to be able to fabricate indium rich group III-nitride alloys and wide band gap group III-nitride compound semiconductors in mutual process conditions. Surface stabilization data suggest that highly volatile compounds such as InN and related alloys can be grown at much higher temperatures if stabilized at high pressures.[5,6] In order to stabilize InN growth at elevated temperatures, a high-pressure chemical vapor deposition (HPCVD) system has been established at GSU.[6–9] The HPCVD reactor can be operated at pressure up to 100 bars to control the decomposition of InN (Refs. 7, 9, and 10) which is an essential step for improving the material quality and for the fabrication of indium rich group III-nitride alloys. The details of the HPCVD system has been described elsewhere.[11,12]

The aim of this study is to investigate the optical properties of InN films grown by HPCVD. Raman, IR-reflectance, and transmission spectroscopy techniques have been applied for the optical characterization. The spectra obtained from IR-reflectance and Raman measurements have been analyzed to estimate free electron concentration. The free carrier concentrations of InN layers are found to be changing from 10^{18} to low 10^{20} cm^{-3}. The optical absorption edge energy calculated from the transmission spectra is 1.2 eV for samples of lower electron concentration. An assessment of the crystalline quality of the layers,[13,9] is given through the line shape analysis of E_2 (high) mode in the Raman spectra.

II. EXPERIMENTAL METHODS

The InN layers analyzed in this contribution were grown on GaN/sapphire and sapphire (0001) substrates by HPCVD, utilizing a horizontal flow channel reactor. The typical sample size is 25×25 mm^2. A pulsed injection scheme is applied to separate the precursors trimethyl-indium (TMI) and ammonia (NH_3). The gas phase chemistry and the surface chemistry processes are monitored real time by UV absorption spectroscopy and principal angle reflectance spectroscopy. Laser light scattering is used to monitor changes in surface roughness real time. Boil-off liquid nitrogen (99.995% purity) is used as a carrier gas during the growth process. A "nanochem" purifier is placed in N_2 supply line in order to reduce the "oxygen" contamination. The total gas flow through the reactor is kept constant during the growth. For the InN layers discussed, the reactor pressure was 15 bars with a total gas flow of 12 slm (standard liters per minute). The precursor flow ratio has been evaluated for molar ratio ammonia to TMI from 600 to 1500 in the growth temperature regime of 1050–1100 K. GaN/sapphire templates used were grown by metal-organic chemical vapor deposition.[9] A two-step growth method was used to grow the InN layers by adjusting temperature, time, and V/III ratio during the initial nucleation period and a steady state growth afterwards.[14]

The Raman spectra of the InN layers were obtained in backscattering geometry $z(\cdots)z$ using excitation energy of 2.33 eV at room temperature. The spectra are normalized to

[a]Electronic mail: malevli@student.gsu.edu

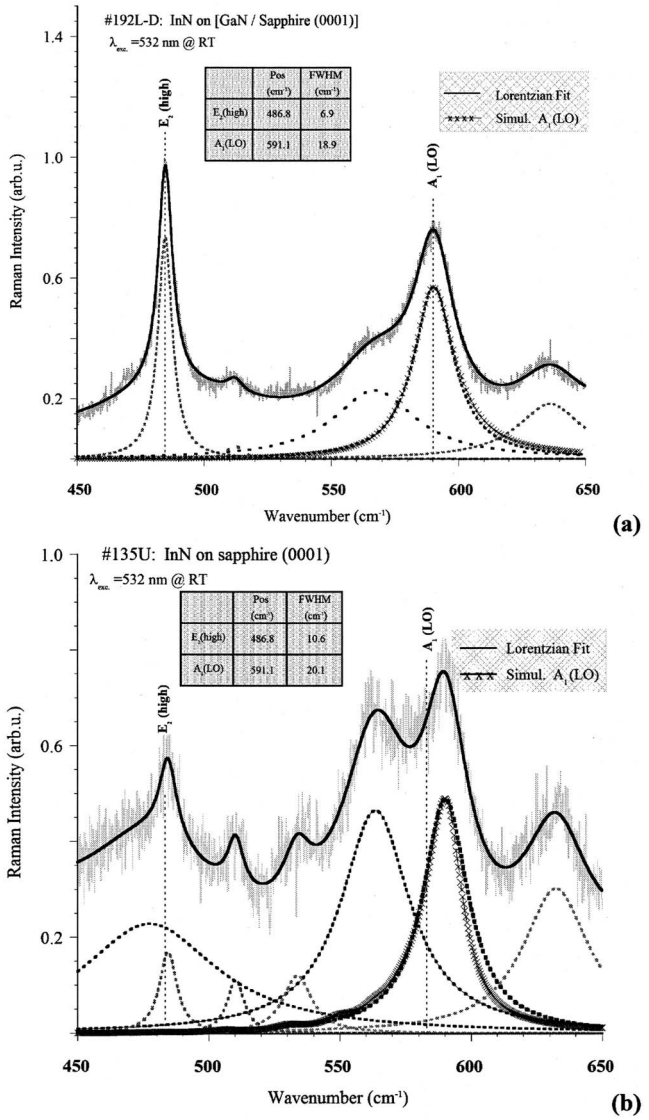

FIG. 1. IR reflectance spectra of sample No. 192 and fitted value for InN film with two different regimes.

intensity of the E_2 (high) line. The IR reflection spectroscopy measurements were performed at room temperature in the energy range of 0.062–0.744 eV under near normal incidence geometry by using a Perkin-Elmer system 2000 fast Fourier transformed and the Graesby optical reflection accessory setup (less than 8° incidence angle). Room temperature transmission spectroscopy measurements were performed with a custom build near-infrared-visible-UV spectrometer (0.443–4.133 eV), which consists of a triple-grating $\frac{1}{2}$ m monochromator with phase-sensitive signal detection and processing.

III. RESULTS AND DISCUSSION

The two allowed optical phonon modes of hexagonal InN are E_2 (high) and A_1 (LO) for Raman in backscattering geometry. These modes were analyzed to evaluate the structural quality and to estimate free carrier concentration in the layers. The peak positions of the observed E_2 (high) and A_1 (LO) are in good agreement with that of predicted as 486 and 591 cm^{-1}, respectively, by Davydov and Klochikhin.[3] The line shape of E_2 (high) is related to structural defects and impurities in GaN structures. Wei *et al.*[15] used this relation as a valuation method for expressing crystalline quality, and they concluded that the E_2 (high) line of full width at half maximum (FWHM) of 4 cm^{-1} indicated a superior crystalline quality material. FWHM of the E_2 (high) line in sample No. 192L is 6 cm^{-1} exhibiting high crystalline quality.[2] Due to the nonpolar character of the E_2 (high) mode, there is no interaction of this mode with the conduction-band electrons.[16] On the other hand, the A_1 (LO) mode interacts with free carriers resulting in broadening of the line shape. In order to estimate free carrier concentration, the observed line shape of A_1 (LO) mode damped by free electrons is simulated by using Linhard-Mermin approach.[17] DP+EO is considered as the major light scattering mechanism within the interaction. The intensity of scattered light is calculated by integrating spectral line shape function up to maximum wave-vector limit by weight factor due to Yukawa-type impurity potential. Figure 1 experimentally shows obtained Raman spectra and simulated A_1 (LO) peak for InN layers grown on sapphire (sample No. 135U) and grown on GaN (sample No. 192L). The general form of the dielectric function used for numerical calculations is given by[17,18]

$$\varepsilon(q,\omega)=\varepsilon_\infty\left(1+\frac{\omega_L^2-\omega_T^2}{\omega_T^2-\omega^2-i\omega\gamma_p}+\frac{(1+i\Gamma_e/\omega)\chi_e^0(q,\omega+i\Gamma_e)}{1+(i\Gamma_e/\omega)\{\chi_e^0(q,\omega+i\Gamma_e)/\chi_e^0(q,0)\}}\right), \quad (1)$$

where Γ_e corresponds to electron damping constant and $\chi_e^0(q,\omega)$ is the temperature dependent Lindhard susceptibility. The plasma frequency has been obtained from IR reflection analysis and used in Raman simulations for a better compatibility of results with those from IR reflection simulations. The theoretical background used to describe the behavior of the LO mode is described in detail elsewhere.[10,17] Figure 2 illustrates the estimated free carrier concentrations calculated from plasmon-phonon coupling as a function of optical absorption edge calculated from optical transmission spectra analysis. The optical absorption edge behavior versus the free carrier concentration shows an exponential behavior in the free carrier concentration range of 10^{+17} $cm^{-3} < n_e < 10^{+20}$ cm^{-3}. The estimated band gap energy is slightly higher than the reported ~0.8 eV which is expected for samples of free carrier concentration in the order of ~10^{+18} cm^{-3}.

In IR reflection spectra of InN, from interference fringes observed in the transparent region above the plasma frequency, the thickness of the layer is calculated. Using a multilayer stack model, the infrared reflection spectra of sample No. 192L could only be modeled by assuming two InN layers with different thicknesses and doping levels, as shown in Fig. 3 and Table I. A Levenberg-Marquardt fitting algorithm is used, where the model parameters are varied until a close fit between calculated and experimental data

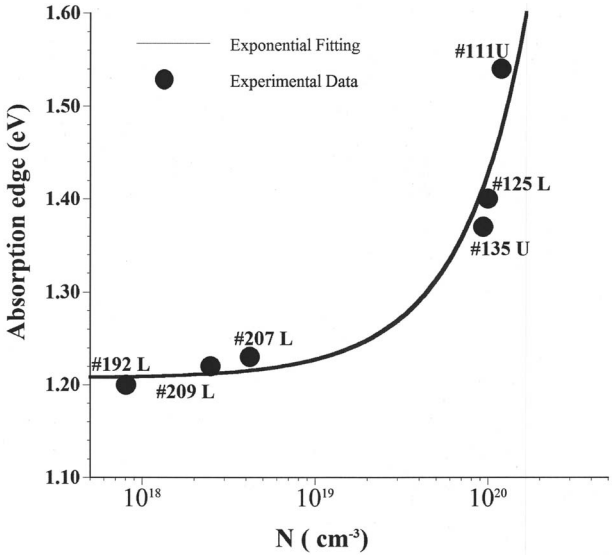

FIG. 2. Optical absorption edge vs free carrier concentration.

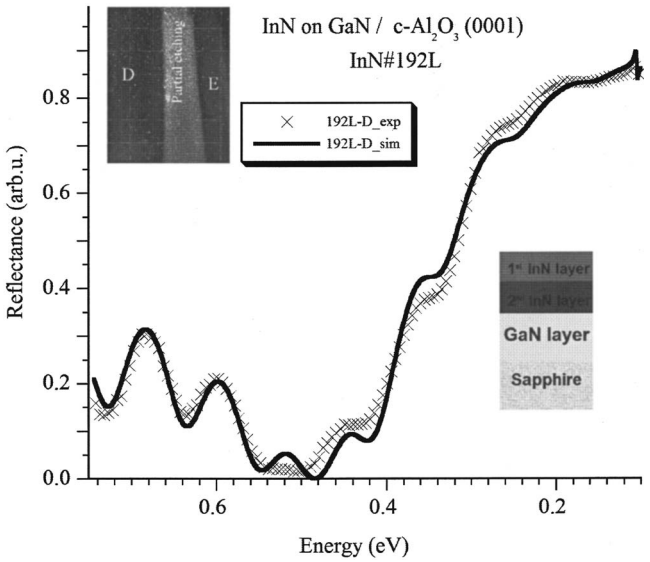

FIG. 3. IR reflectance spectra of sample No. 192 and fitted value for InN film with two different regimes.

was found.[19] The effective electron mass of InN is set constant to $0.09m_0$ (Ref. 20) by neglecting the first order dependency of the electron mass with free carrier concentration. The best-fit approximation of the infrared reflection spectra reveals the plasma frequency ω_p and the plasma damping constant γ_p. The plasma parameters ω_p and γ_p are related to the concentration N_e, the effective mass m_e, and the mobility μ_e of the free electrons by following equations:

$$\omega_p^2 = \frac{N_e q^2}{m_e \varepsilon_0 \varepsilon_\infty}, \tag{2}$$

$$\gamma_p = \frac{q}{m_e \mu_e}, \tag{3}$$

The details of the calculation method have been published elsewhere.[9] The simulated IR spectra agree well with the experimental data as reproducing the correct interference fringes. The fit results summarized in Table I show estimated free carrier concentration, high frequency dielectric function, thickness and mobility on the layers studied by IR spectra analysis. The required second InN layer for sample Nos. 125L, 192L, and 209L is calculated to have low free carrier concentration (below 1×10^{18} cm^{-3}).

Figure 4 shows the optical transmission spectra of InN samples with the simulated spectra. From the fitting analysis, the optical absorption edge of the InN film layers is found to be from 1.5 to 1.1 eV. The optical transmission spectra are fitted by applying a modified model dielectric function (MDF) model[21] with additional oscillators at ≈0.8 and ≈0.4 eV. This approach provides a good fit of the experimental transmission spectra where the MDF is expressed as

$$\varepsilon'_{\mathrm{InN}}(\omega) = \varepsilon_{\mathrm{InN}} + \sum_{n=1}^{2} \frac{S_{ab}}{[E_{ab}^2 - (h\omega)^2] - ih\omega\Gamma_{ab}}, \tag{4}$$

where S_{ab} is the oscillator strength, E_{ab} is the energetic position of the oscillator, and Γ_{ab} is the damping of the Lorentzian. The best-fit results provide estimation for thickness, high frequency dielectric constant, and optical absorption edge.

The correlation of calculated optical absorption edge of the InN films with the free carrier concentration estimations obtained by IR-reflection spectroscopy is shown in Fig. 5. There is a difference between calculated free carrier concentration from IR reflection and Raman simulations although similar exponential behavior with respect to absorption edge is observed. This difference might be due to the difference on spatial integration (Raman ~0.1 μm, IR reflection ~3 mm) and/or due to different coupling mechanisms between the probe wavelength and free carriers.

TABLE I. Model fitting parameters for IR reflection spectroscopy.

	209L		125L		192L		
	First layer	Second layer	First layer	Second layer	First layer	Second layer	135U
N (cm^{-3})	8×10^{19}	$<1\times10^{18}$	1×10^{20}	$<5\times10^{17}$	6×10^{19}	$<1\times10^{18}$	1.2×10^{20}
ε_∞	8	7.5	7.5	7.3	6.5	7.5	7.6
d (nm)	415	120	393	79	452	81	320
μ (cm^2 V^{-1} s^{-1})	250	>500	266	NA	225	NA	211

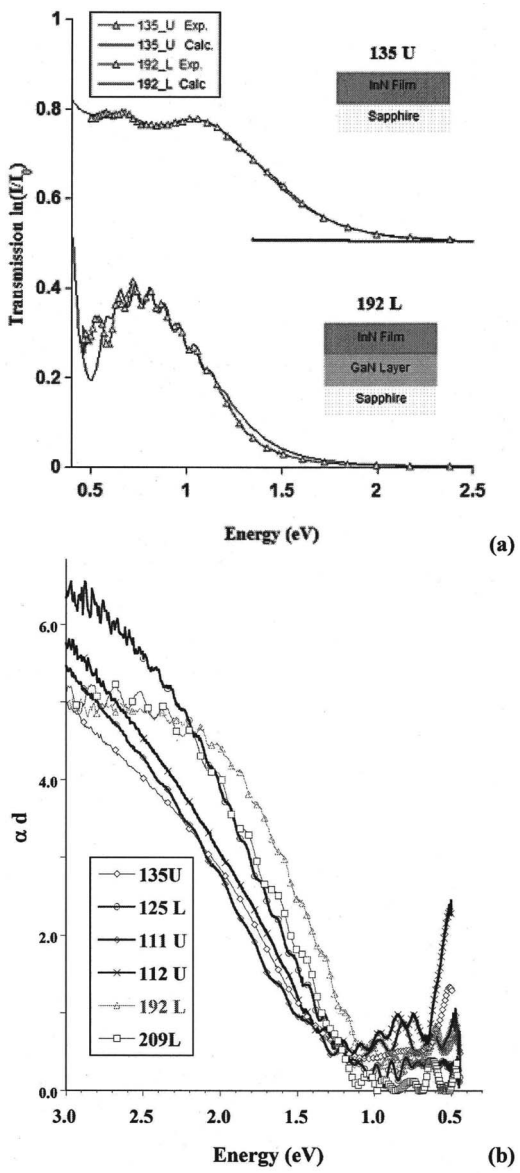

FIG. 4. (a) Transmission spectra and their best fits for InN layers deposited on sapphire and GaN/sapphire substrates. (b) Optical absorption edge with for different electron concentrations.

IV. CONCLUSION

InN layers grown by HPCVD were investigated by Raman, infrared reflectance, and transmission spectroscopy. The spectra where analyzed to extract the free electron concentrations and correlated to optical absorption edge obtained from optical transmission spectra analysis practicing a *modified model dielectric function*. An exponential dependence is observed between optical absorption edge and free carrier concentration. In IR reflection spectra analysis, a two layer model had to be applied, which indicate the existence of a surface layer with a higher free carrier concentration than that of inner layer.

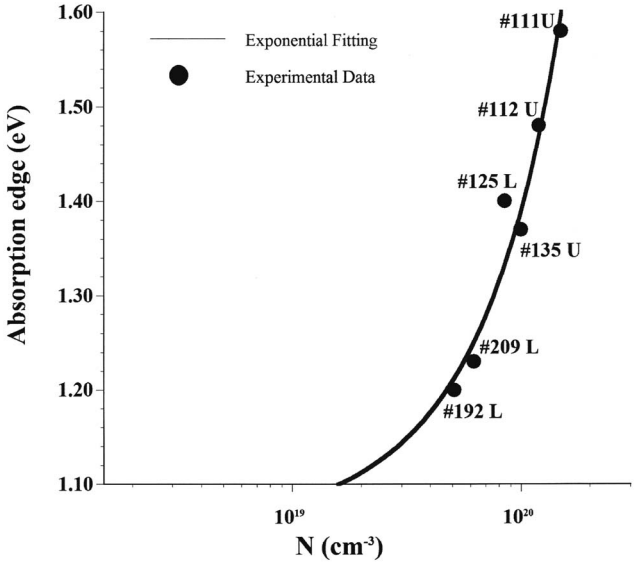

FIG. 5. Dependence of optical absorption edge on carrier concentration as obtained from modified model dielectric function approach in combination with experimental data.

ACKNOWLEDGMENTS

The authors would like to acknowledge support of this work by AFOSR Grant No. FA9550-07-1-0345.

[1]A. G. Bhuiyan, A. Hashimoto, and A. Yamamoto, J. Appl. Phys. **94**, 2779 (2003).
[2]K. S. A. Butcher and T. L. Tansley, Superlattices Microstruct. **38**, 1 (2005).
[3]V. Y. Davydov and A. A. Klochikhin, Semiconductors **38**, 861 (2004).
[4]S. Nakamura, S. Masayuki, and T. Mukai, Jpn. J. Appl. Phys., Part 2 **32**, L8 (1993).
[5]J. MacChesney, P. M. Bridenbaugh, and P. B. O'Connor, Mater. Res. Bull. **5**, 783 (1970).
[6]N. Dietz, in *III-Nitrides Semiconductor Materials*, edited by Z. C. Feng (Imperial College Press, 2006), pp. 203–255.
[7]N. Dietz, M. Strassburg, and V. Woods, J. Vac. Sci. Technol. A **23**, 1221 (2005).
[8]V. Woods and N. Dietz, Mater. Sci. Eng., B **127**, 239–250 (2006).
[9]M. Alevli, G. Durkaya, W. Fenwick, A. Weerasekara, V. Woods, I. T. Ferguson, A. G. U. Perera, and N. Dietz, Appl. Phys. Lett. **89**, 112119 (2006).
[10]M. Alevli *et al.*, Mater. Res. Soc. Symp. Proc. **955E**, 1 (2007).
[11]B. H. Cardelino, C. E. Moore, C. A. Cardelino, and N. Dietz, Proc. SPIE **5912**, 86 (2005).
[12]N. Dietz, V. Woods, S. McCall, and K. J. Bachmann, Proceedings of the Microgravity Conference, NASA/CP-2003–212339, 2003, pp. 169–181.
[13]V. Y. Davydov *et al.*, Appl. Phys. Lett. **75**, 3297 (1999).
[14]N. Dietz, M. Alevli, V. Woods, M. Strassburg, H. Kang, and I. T. Ferguson, Phys. Status Solidi B **242**, 2985 (2006).
[15]T. B. Wei, R. F. Duan, J. X. Wang, J. M. Li, Z. Q. Huo, P. Ma, Z. Liu, and Y. P. Zeng, J. Phys. D **40**, 2881 (2007).
[16]J. S. Thakur, D. Haddad, V. M. Naik, R. Naik, G. W. Auner, H. Lu, and W. J. Schaff, Phys. Rev. B **71**, 115203 (2005).
[17]F. Demangeot, C. Pinquier, J. Frandon, M. Gaio, O. Briot, B. Maleyre, S. Ruffenach, and B. Gil, Phys. Rev. B **71**, 104305 (2005).
[18]U. Fano, Phys. Rev. **124**, 1866 (1961).
[19]I. Wu Appl. Phys. Lett. **84**, 2805 (2004).
[20]T. Inushima, M. Higashiwaki, and T. Matsui, Phys. Rev. B **68**, 235204 (2003).
[21]T. Kawashima, H. Yoshikawa, S. Adachi, S. Fuke, and K. Ohtsuka, J. Appl. Phys. **82**, 3528 (1997).